Atomic and electronic structures of $SrTiO_3$/GaAs heterointerfaces: An 80-kV atomic-resolution electron energy-loss spectroscopy study

Q. Qiao, R. F. Klie, and S. Öğüt
University of Illinois at Chicago, Chicago, Illinois 60607, USA

J. C. Idrobo
Materials Science and Technology Division, Oak Ridge National Laboratory, Oak Ridge, Tennessee 37831, USA
(Received 4 October 2011; revised manuscript received 22 March 2012; published 3 April 2012)

We have examined the atomic and electronic structures of epitaxially grown, ultrathin $SrTiO_3$ (100) films on GaAs (001) using 80-kV aberration-corrected atomic-resolution Z-contrast imaging and electron energy-loss spectroscopy (EELS) to develop a fundamental understanding of the interfacial structure-property relationships. We find that the interface is atomically abrupt and no surface reconstruction of the GaAs (001) surface is observed. Using atomic-column resolved EELS, we examine the oxygen vacancy and Ti concentrations in the $SrTiO_3$ film and across the heterointerface. We show that Ti diffuses into the first few monolayers of GaAs. Using a combination of EELS and first-principles calculations, we present evidence for the formation of As oxides at the interface depending on the thin-film growth conditions. These findings are used to explain the differences in the transport behavior of the films.

DOI: 10.1103/PhysRevB.85.165406 PACS number(s): 68.37.Ma, 79.20.Uv, 77.55.−g

Crystalline complex oxide thin films on semiconductor substrates have emerged as an alternative to SiO_2 based technologies in fabricating the metal-oxide-semiconductor field-effect transistors (MOSFETs) because such complex oxides can act as effective insulators without compromising the thickness of the film. These materials can be studied with a variety of experimental and theoretical tools.[1] Compound semiconductors have also been considered for replacing silicon channel due to better electron mobilities and velocities.[2] In addition, over the past few years, ultrathin metal-oxide films on polar semiconductor surfaces have received much attention due to the emergence of novel interfacial phenomena, including ferroelectricity, superconductivity, and the presence of an interfacial two-dimensional electron gas.[3–6] For more than two decades now, various techniques have been used to achieve a layer-by-layer crystalline oxide film deposition, including pulsed laser deposition and molecular beam epitaxy (MBE), in an effort to avoid the formation of the amorphous layer at the interface.[7,8]

The synthesis of single-crystalline $SrTiO_3$ (STO) films on polar semiconducting GaAs using MBE was first reported by Liang *et al.*[9,10] These STO/GaAs interfaces were then characterized using atomic-resolution Z-contrast imaging and x-ray photoemission spectroscopy,[11] as well as preliminary first-principles density functional theory (DFT) calculations in an effort to obtain a fundamental understanding of the structural and electronic properties.[12,13] It has been reported that the film prefers to be SrO terminated at the interface, regardless of the growth conditions, and a submonolayer of Ti between the oxide and semiconductor can relieve the Fermi-level pinning after the completion of the thin-film deposition. Because of the sensitivity of the STO/GaAs interface to the high-energy electron beam, it was not possible to perform atomic-resolution electron energy-loss spectroscopy (EELS) at the time.[11] Accordingly, a detailed understanding of the electronic structures at the interface is still missing. Until recently, atomic-resolution imaging and spectroscopy at primary energies less than 100 kV was not possible. However, advances in instrumentation design now allow for such characterization to be performed at electron energies as low as 60 kV.[14] In this paper, we show atomic-scale studies of STO/GaAs interfacial structures by utilizing atomic-resolution Z-contrast imaging and EELS in aberration-corrected scanning transmission electron microscopy (STEM) operated at an acceleration voltage of 80 kV. We combine these experimental results with first-principles computations for O K edges to help understand the interfacial atomic and electronic structures.

As reported by Klie *et al.*[11] the STO thin films were grown on the As-terminated p-GaAs (001) by MBE with atomic-layer precision using two types of growth methods. In the first method, one half-monolayer of Ti was deposited on the GaAs substrate before the STO deposition (*sample 1*); in the second, the As-stabilized GaAs surface was exposed to the evaporated Sr and Ti under a controlled oxygen pressure (*sample 2*).[9] The experimental data were obtained using the aberration-corrected JEOL JEM-ARM200CF STEM/TEM equipped with a cold field-emission source, which yields an energy resolution of 0.35 eV when operated at 80–200 kV, and a probe spherical-aberration corrector which allows for 1.2 Å spatial resolution in high-angle annular dark-field imaging at 80 kV. The images and EEL spectra were acquired using an acceleration voltage of 80 kV. For atomic-resolution Z-contrast imaging, a collection semiangle from 90 to 170 mrad and a convergence semiangle of 22 mrad were used. For EELS, a convergence angle of 30 mrad and a collection angle of 35 mrad were used. We find that using a primary voltage of 80 kV allows us to reduce the sensitivity of the samples to electron beam damage. In particular, we did not observe any electronic or structural changes in the samples even after their repeated exposure to the electron beam. First-principles calculations within the local density approximation were performed using the projector augmented wave method as implemented in VASP.[15] We used a plane wave cutoff energy of 300 eV. Integrations in reciprocal space were performed by the Monkhorst-Pack scheme with a $12 \times 12 \times 12$ mesh for

 ©2012 American Physical Society

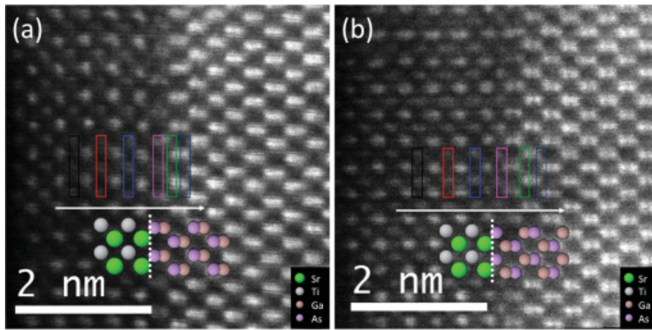

FIG. 1. (Color online) High-resolution Z-contrast image of STO/GaAs interface of (a) *sample 1* (with Ti prelayer) showing STO [010]||GaAs [110] epitaxy and (b) *sample 2* (without Ti prelayer) showing STO [100]||GaAs [$1\bar{1}0$] epitaxy. The colored rectangles highlight the individual scan areas, the proposed atomic columns of the interface are shown as insets at the bottom, and the dotted lines mark the interface between the thin film and the As terminated substrate.

perovskite STO, a 6 × 12 × 4 mesh for monoclinic claudetite As_2O_3, and a 6 × 6 × 6 mesh for cubic arsenolite As_2O_3, with 5, 20, and 80 atoms in the unit cell, respectively.

Figures 1(a) and 1(b) show the high-resolution Z-contrast image of the *sample 1* and *sample 2*. The colored rectangles highlight the individual scan areas. The proposed model of the atomic arrangement at the interface is shown as an inset in both micrographs. The dotted lines mark the interface between the STO thin film and the As-terminated GaAs substrate. Figure 1(a), with the STO [010]||GaAs [110] epitaxy, shows a sharp interface with SrO layer of the thin film in perfect registry with the As-terminated substrate, providing no evidence of the Ti prelayer presence at the interface. It is also interesting to note here that the interface appears abrupt and no surface reconstruction of the GaAs (001) surface is observed. Figure 1(b), with the STO [100]||GaAs [$1\bar{1}0$] epitaxy, shows the interface of the thin film deposited without Ti pretreatment, also bearing no mark of any surface reconstruction on the substrate.

We point out that while several previous studies on bare, As-terminated GaAs (001) surfaces have found the (2×4)-$\beta2$ surface reconstruction to be energetically favorable,[16–19] it appears that the STO deposition eliminates this surface reconstruction as inferred from our Z-contrast images.[11] These findings are consistent with a previous Z-contrast imaging study, which showed that the STO films with and without the Ti prelayer appear to be structurally identical.[11] However, in that previous study, Klie *et al.*[11] were not able to explain the observed differences in the electronic properties of the two samples, since atomic-resolution EELS was not possible at 300 kV.

In this study, using an 80-kV electron beam, we can now explore the interfacial electronic structure using atomic-resolution EELS spectrum imaging of the Ti L and O K edges. The acquired Ti L edges of *sample 1* and *sample 2* are shown in Figs. 2(a) and 2(b), respectively. The spectra were calibrated with respect to the O K-edge onset at 532 eV. The uppermost spectrum shows a reference taken from bulk STO, which provides the near-edge fine structures for Ti^{4+}. Each of

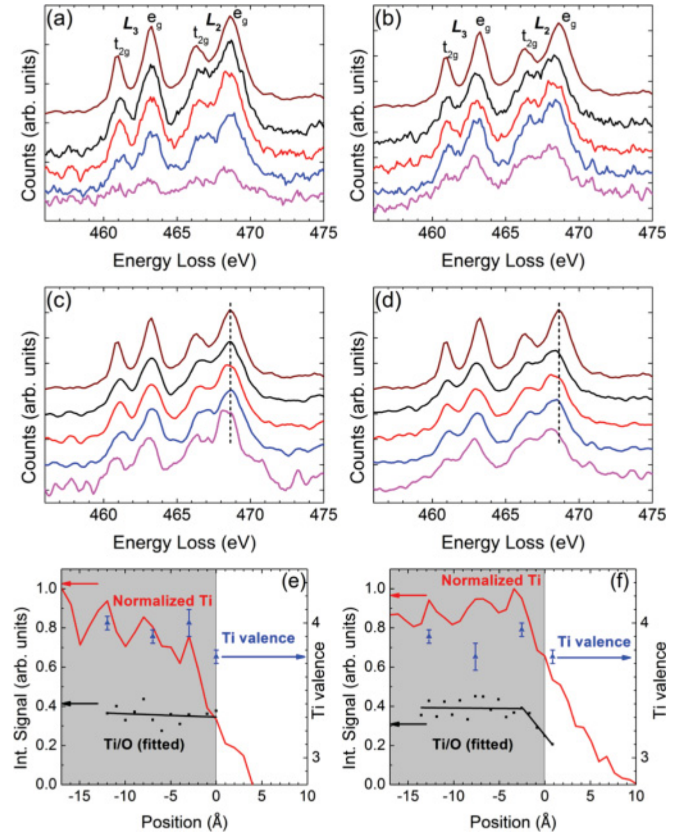

FIG. 2. (Color online) Background subtracted Ti L edges of (a) *sample 1* and (b) *sample 2*. The top spectrum is taken from bulk STO; each of the other colored spectra corresponds to the signal enclosed by the corresponding rectangle superimposed on the image in Fig. 1. Ti L-edge fine structure spectra fitted to its second nearest neighbor and normalized for (c) *sample 1* and (d) *sample 2*. (e) and (f) show the normalized intensity of Ti signal, the linearly fitted Ti/O ratio, and the quantified Ti valence of *sample 1* and *sample 2*, respectively. The shaded area indicates the STO film.

the other colored spectra corresponds to the signal enclosed by the corresponding rectangle superimposed on the image in Figs. 1(a) and 1(b), providing the average information of the enclosed area. Figures 2(a) and 2(b) show the background subtracted Ti L-edge fine structure of the STO/GaAs interface with and without Ti prelayer, respectively. The crystal field splitting of Ti L_3 and L_2 edges can be resolved, which is similar to the reported Ti^{4+} fine structure.[20] However, it is worth noticing that both the L_3 and L_2 edges are shifted to lower energies at the interface. As demonstrated earlier, such a chemical shift indicates a decrease of the Ti valence,[20,21] in this case, at the interface.

Each of the acquired Ti L-edge fine structure spectra is then fitted to its second nearest neighbor (by taking the average over the two adjacent points in both the forward and backward directions for each pixel in the Ti L-edge spectrum) and normalized in Fig. 2(c) for *sample 1*, and in Fig. 2(d) for *sample 2*. We compare the Ti L-edge spectra acquired across the interface with the previous result acquired from bulk STO[22] in order to quantify the Ti valence change at the interface. In Fig. 2(c), the film deposited with the Ti prelayer, both the Ti L_3 and L_2 edges shift to lower energies as the electron

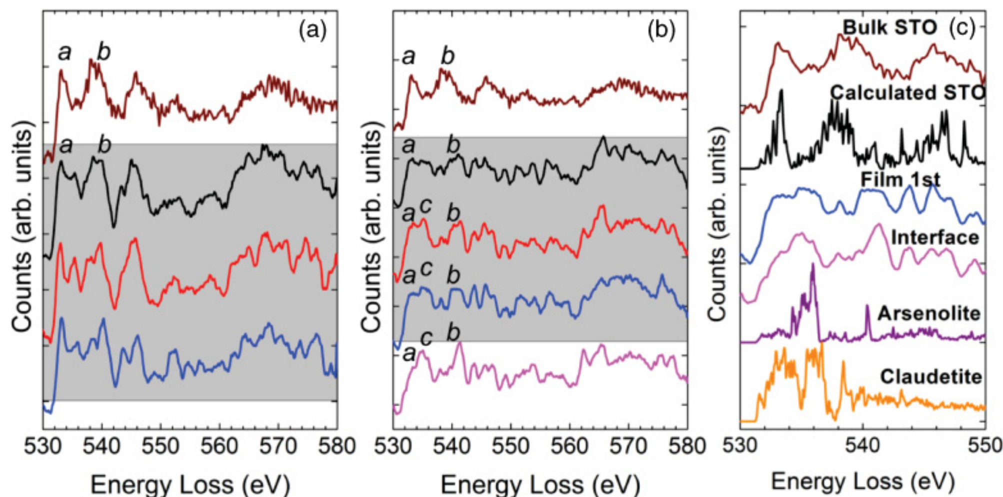

FIG. 3. (Color online) O K edges of (a) *sample 1* and (b) *sample 2* (obtained from the same positions as the Ti L edges) fitted to their fifth nearest neighbors and compared with the previous results on bulk STO. The shaded area indicates the STO film. (c) O K edges and O 2p unoccupied density of states in bulk STO, O K edges of *sample 2* films, and O 2p density of unoccupied states in As_2O_3.

probe approaches the interface from the STO film, indicating a decrease of the Ti valence from 4+ to a mixture of 3+ and 4+.[20] This decrease in Ti valence could be due to either the presence of interfacial oxygen vacancies, or because Ti forms bonds with As rather than O at the interface. The chemical shift of Ti L_2 edge is marked in the figure, and quantified assuming a linear relationship between the Ti valence and the L_2-edge chemical shift.[21] The same method is used in the valence quantification for *sample 2*, where a decrease in the Ti valence is also measured as a function of distance from the heterointerface.

In Figs. 2(e) and 2(f), the normalized intensity of Ti signal is obtained by integrating the background subtracted Ti L_3 and L_2 edges in the energy range of 455–475 eV. The shaded area indicates the STO film, while the white area indicates the GaAs substrate. This Ti intensity oscillates according to the atomic structure of the STO film layer-by-layer, but exhibits a reduction at the interface. However, the Ti signal remains detectable ~0.4 nm into the substrate GaAs in *sample 1*, and ~0.7 nm in *sample 2*. We point out that these reported differences in the Ti profile are not observed in the O concentration profiles. This is important, since an increased sample thickness could result in signal delocalization of similar magnitude as reported in our experiments. However, any such delocalization should not be limited to the Ti L-edge signal, but also measurable in the O K-edge profile, which we did not find. We can, therefore, conclude that the Ti signal in the GaAs substrate is solely due to Ti diffusion into the first few monolayers of GaAs regardless of the thin-film growth condition GaAs, and not an imaging artifact.

The integrated Ti/O-signal ratio is also measured and linearly fitted for both samples using an energy window between 530 eV and 550 eV for the O K edge. It is interesting to notice that the Ti/O ratio in *sample 1* remains steady, but shows a significant decrease at the interface of *sample 2*. Such a change in *sample 2* (i.e., the sample without the Ti prelayer) indicates a reduction of Ti concentration at the interface, which supports the fact that there is no interfacial Ti prelayer and Ti diffuses further into the subsurface GaAs than in *sample 1*, thereby leaving behind a Ti poor layer of STO at the GaAs interface.

As mentioned above, the Ti valence exhibits a decrease at the interface in both samples, suggesting an increase of oxygen vacancy concentration, and/or a different bonding state at the STO/GaAs interface. By comparing the Ti valence at equal distances from the interface for both films, we suggest that in *sample 2* the STO film is more oxygen deficient than in *sample 1*. In fact, we find that the average Ti valence in the STO film in *sample 1* is 4+, while the average Ti valence in the STO film of *sample 2* is 3.8+. The fact that *sample 2* has more oxygen vacancies in the film, but lower Ti/O-intensity ratio at the interface can be understood if we assume that O is bonded with As rather than Ti at the interface. This explains the increased presence of oxygen at the heterointerface as well as the oxygen deficiency in the STO film of *sample 2* compared to that of *sample 1*. Our conclusions are consistent with some of the earlier studies on the oxidation of GaAs substrates, which attributed Fermi level pinning to arsenic oxides at the interface.[23–25] Moreover, in previous studies where thermal reactions in the Ti/GaAs system were studied to understand the metallization of the semiconductor surface, it was found that interfacial layers consisting of Ti-Ga and Ti-As are formed on the Ti film surface.[26–28]

In Figs. 3(a) and 3(b), the acquired O K edges (obtained from the same positions as the Ti L edges) are fitted to their fifth nearest neighbors for *samples 1* and *2*, respectively, and compared with the previous results for bulk STO. The colored spectra correspond to the colored rectangles in Figs. 1(a) and 1(b), while the shaded area indicates the STO film. In contrast to the Ti intensity, the oxygen signal becomes undetectable at the interface between the ultrathin film and the substrate, while the Ti signal remains observable, as shown in Figs. 2(a) and 2(b). It is clearly noticeable from the O K-edge spectra that the electronic structures at the interface in *sample 1* and *sample 2* are different. More specifically, in *sample 1* (with the Ti prelayer), all three spectra in the film bear the same features,

similar to the O signal acquired in bulk STO, shown on the top of Fig. 3(a). In *sample 2* (without Ti prelayer), a new peak arises at 536 eV in the O K-edge fine structure at the interface, and disappears after two unit cells into the film. Similar to Fig. 3(a), peaks a and b display the t_{2g}-e_g final state splitting,[29] while the new peak c suggests a change in the coordination of O at the interface of *sample 2*, compared to that in bulk STO, which we attribute to the formation of As-O bonds. This suggestion is consistent with our observations on O and Ti concentrations and Ti/O-intensity ratios mentioned earlier. First-principles calculations summarized below provide further evidence for the validity of this suggestion.

First-principles calculations within the framework of DFT were performed on bulk STO and various As_2O_3 compounds in order to understand the emergence of this peak. The results are shown in Fig. 3(c), where the computed O $2p$ partial densities of unoccupied states are compared with the experimental EEL spectra. We note that the DFT calculations for bulk STO successfully capture all the main peaks observed in the experimental spectrum over a 20-eV energy range. Furthermore, the new peak observed at 536 eV in the STO/GaAs interfacial spectrum agrees very well with the features observed in As_2O_3, in its arsenolite and claudetite polymorphs. These findings strongly support our hypothesis that As oxides form at the interface in *sample 2*, which is responsible for the measured Fermi-level pinning.

By combining these experimental results with the previous studies on the thermal reactions in the metallization and oxidation of GaAs, a likely scenario of the metal-oxide thin-film deposition can be summarized as follows. In *sample 1*, after the Ti prelayer deposition at approximately 300 °C, Ti breaks up the As dimers on the GaAs (2×4)-$\beta2$ surface,[30] and eliminates the surface reconstruction of the substrate. The resulting Ti-As bonds shift the As $3d$ core-level position and induce Fermi-level pinning. After the oxide growth temperature is increased to 550 °C to improve the crystallinity of the STO film, the surface-bonded Ti penetrates into the substrate, which alleviates the Fermi-level pinning. In *sample 2*, without the presence of the Ti prelayer, the As surface layer gets oxidized when the STO deposition begins, and these arsenic oxides at the interface are responsible for the Fermi level pinning. This is also the reason for the observed differences in the O K-edge fine structure at the STO/GaAs interface in *sample 2*.

In summary, we have presented a combination of atomic-resolution Z-contrast imaging, atomic-column resolved EELS at 80 kV, and first-principles DFT studies to examine the atomic and electronic structures of the interface between single crystalline STO and semiconducting GaAs. As in previous studies, we have found no evidence of a Ti prelayer or any reconstruction on the GaAs side of the interface after the thin-film deposition using Z-contrast imaging. Our present atomic-resolution EELS studies have indicated that Ti diffuses into subsurface GaAs, the extent of which depends on the film growth conditions. Furthermore, our detailed analysis of the near-edge fine structure as a function of position from the interface has revealed a shift toward lower energies in the Ti L_2 edges at the STO/GaAs interface and different bonding configurations, supported by first-principles DFT calculations, at the interface resulting from different growth methods. Our results suggest that although it does not affect the cationic arrangement at the interface, the Ti prelayer deposition alleviates the oxidation of the substrate and consequently the Fermi-level pinning at the interface, an effect which will be essential in further improving the performance of single crystal oxides in MOSFET devices.

This work was supported by the National Science Foundation Grant No. DMR-0846748 (Q.Q. and R.F.K) and by Oak Ridge National Laboratory's Shared Research Equipment (ShaRE) User Program, which is sponsored by the Office of Basic Energy Sciences, US Department of Energy (J.C.I). S.Ö. acknowledges partial support from DOE Grant No. DE-FG02-09ER16072 and support from the National Science Foundation under the Independent Research/Development program while working at the Foundation. This research used resources of NERSC, which is supported by the Office of Science of the US Department of Energy. The UIC JEOL JEM-ARM200CF is supported by a MRI-R^2 grant from the National Science Foundation (Grant No. DMR-0959470).

[1] J. W. Reiner, A. M. Kolpak, Y. Segal, K. F. Garrity, S. Ismail-Beigi, C. Ahn, and F. J. Walker, Adv. Mater. **22**, 2919 (2010).

[2] M. Hong, J. Kwo, A. R. Kortan, J. P. Mannaerts, and A. M. Sergent, Science **283**, 1897 (1999).

[3] C. H. Ahn, K. M. Rabe, and J. M. Triscone, Science **303**, 488 (2004).

[4] J. H. Haeni, P. Irvin, W. Chang, R. Uecker, P. Reiche, Y. L. Li, S. Choudhury, W. Tian, M. E. Hawley, B. Craigo, A. K. Tagantsev, X. Q. Pan, S. K. Streiffer, L. Q. Chen, S. W. Kirchoefer, J. Levy, and D. Schlom, Nature (London) **430**, 758 (2004).

[5] J. C. Woicik, H. Li, P. Zschack, E. Karapetrova, P. Ryan, C. R. Ashman, and C. S. Hellberg, Phys. Rev. B **73**, 024112 (2006).

[6] M. P. Warusawithana, C. Cen, C. R. Sleasman, J. C. Woicik, Y. L. Li, L. F. Kourkoutis, J. A. Klug, H. Li, P. Ryan, L. P. Wang, M. Bedzyk, D. A. Muller, L. Q. Chen, J. Levy, and D. G. Schlom, Science **324**, 367 (2009).

[7] E. J. Tarsa, M. Degraef, D. R. Clarke, A. C. Gossard, and J. S. Speck, J. Appl. Phys. **73**, 3276 (1993).

[8] M. G. Blamire, J. L. MacManus-Driscoll, N. D. Mathur, and Z. H. Barber, Adv. Mater. **21**, 3827 (2009).

[9] Y. Liang, J. Kulik, T. C. Eschrich, R. Droopad, Z. Yu, and P. Maniar, Appl. Phys. Lett. **85**, 1217 (2004).

[10] Y. Liang, J. Curless, and D. McCready, Appl. Phys. Lett. **86**, 082905 (2005).

[11] R. F. Klie, Y. Zhu, E. I. Altman, and Y. Liang, Appl. Phys. Lett. **87**, 143106 (2005).

[12] J. Wang, X. S. Wu, and D. Bai, Europhys. Lett. **86**, 46008 (2009).

[13] Q. Qiao, W. Walkosz, S. Ogut, and R. F. Klie, APS March Meeting, 2010.

[14] O. L. Krivanek, M. F. Chisholm, V. Nicolosi, T. J. Pennycook, G. J. Corbin, N. Dellby, M. F. Murfitt, C. S. Own, Z. S. Szilagyi, M. P. Oxley, S. T. Pantelides, and S. J. Pennycook, Nature(London) **464**, 571 (2010).

[15] G. Kresse and J. Furthmuller, Phys. Rev. B **54**, 11169 (1996).
[16] D. J. Chadi, J. Vac. Sci. Technol. A **5**, 834 (1987).
[17] M. D. Pashley, Phys. Rev. B **40**, 10481 (1989).
[18] W. G. Schmidt and F. Bechstedt, Phys. Rev. B **54**, 16742 (1996).
[19] V. P. LaBella, H. Yang, D. W. Bullock, P. M. Thibado, P. Kratzer, and M. Scheffler, Phys. Rev. Lett. **83**, 2989 (1999).
[20] D. A. Muller, N. Nakagawa, A. Ohtomo, J. L. Grazul, and H. Y. Hwang, Nature (London) **430**, 657 (2004).
[21] M. Sankararaman and D. Perry, J. Mater. Sci. **27**, 2731 (1992).
[22] R. F. Klie, C. Johnson, and Y. M. Zhu, Microscopy Microanal. **14**, 104 (2008).
[23] M. M. Frank, G. D. Wilk, D. Starodub, T. Gustafsson, Y. J. Garfunkel, E. Chabal, J. Grazul, and D. A. Muller, Appl. Phys. Lett. **86**, 152904 (2005).
[24] M. L. Huang, Y. C. Chang, C. H. Chang, Y. J. Lee, P. Chang, J. Kwo, T. B. Wu, and M. M. Hong, Appl. Phys. Lett. **87**, 252104 (2005).
[25] D. I. Garcia-Gutierrez, D. Shahrjerdi, V. Kaushik, and S. K. Banerjee, J. Vac. Sci. Technol. A **27**, 2390 (2009).
[26] O. Wada, S. Yanagisawa, and H. H. Takanashi, Appl. Phys. Lett. **29**, 263 (1976).
[27] R. R. Ludeke and G. Landgren, Phys. Rev. B **33**, 5526 (1986).
[28] M. Kniffin and C. R. Helms, J. Vac. Sci. Technol. A **5**, 1511 (1987).
[29] L. A. Grunes, R. D. Leapman, C. N. Wilker, R. Hoffmann, and A. B. Kunz, Phys. Rev. B **25**, 7157 (1982).
[30] Q. Qiao, R. F. Klie, and S. Ogut (unpublished).